Available online at www.sciencedirect.com
SCIENCE DIRECT®
Journal of Power Sources 135 (2004) 267–272
JOURNAL OF POWER SOURCES
www.elsevier.com/locate/jpowsour

Novel liquid lithium borates characterized with high lithium ion transference numbers

Ruoyuan Tao*, Daisuke Miyamoto, Takahiro Aoki, Tatsuo Fujinami

Department of Materials Science, Faculty of Engineering, Shizuoka University, Hamamatsu 432-8561, Japan

Received 2 February 2004; accepted 1 April 2004

Available online 24 June 2004

Abstract

A series of lithium borates with two oligoether chains and two electron withdrawing groups directly bonded to the ate complex center were prepared. Ionic conductivity as high as 4.5×10^{-5} S/cm was achieved at 30 °C for Salt A($n = 7.2$). Lithium borates exhibited much higher ionic conductivities than corresponding lithium aluminates, which was explained by the partial charges on oxygen atoms obtained from MOPAC calculation and by the results of fitting Vogel–Tammann–Fulcher (VTF) equation to conductivity data. Lithium borates also exhibited high lithium ion transference numbers (T^+) and satisfactory electrochemical stabilities. They were considered as promising materials for lithium battery application.

Keywords: Electrolyte; Ionic conductivity; Lithium aluminate; Lithium borate; Lithium ion transference number; Partial charge

1. Introduction

Solid polymer electrolytes are thought of as alternatives to liquid electrolytes due to their high energy densities, good electrochemical and thermal stabilities, easy workability and high safety [1,2]. They are normally obtained by dissolving weak ion pairing lithium salts into polymer matrices. Poly(ethylene oxide) (PEO) is the most studied host polymer because of its high solubility for inorganic salts [3–5]. However, low ionic conductivity at room temperature due to the crystallization of PEO restricts the application of PEO based electrolytes in lithium battery [6,7]. Hyper-branched systems [8,9], cross-linked polymers [10–12], and comb-like polymers [13–15] were developed and worked as host polymers. These polymer electrolytes show high ionic conductivities even at room temperature. But due to the low salt solubility, it is difficult to further increase the concentration of charge carriers in these systems. It should also be noted that these polymer electrolytes are dual-ion conduction systems, lithium ion transference number is usually low, normally <0.4 [16]. A build-up of concentration gradient of ions, i.e. polarization of cell, will be resulted during charge–discharge cycling, which leads to the increase of resistance of electrolyte and other safety problems. Therefore, single ion conducting polymer electrolytes are favored for lithium ion secondary batteries [17]. However, the strong ion pairing between lithium ion and polymer anion greatly depressed the ionic conductivity [18,19]. Recently, it was reported that polysiloxanes containing trifluoromethylsulfonamide anions and oligoether side chains [20], and oxalate capped orthoborates containing polyether chains [21] showed relatively high ionic conductivities ($\geqq 10^{-5}$ S/cm at 30 °C) due to weak ion pairing structures. Our laboratory reported a single ion conducting siloxyaluminate polymer exhibiting the same magnitude of ionic conductivity [22].

In order to obtain a completely amorous lithium ion conducting electrolyte containing a large number of charge carriers as well as high lithium ion mobility, we had bonded oligoether chains and electron withdrawing groups to aluminum to get lithium aluminates. Good performance was observed for this aluminates [23]. In this work, several lithium borates were synthesized. They exhibited much better performance than corresponding lithium aluminates. The relationship between the structures and performance was revealed by the MOPAC calculation and VTF fitting results.

* Corresponding author. Tel.: +81-53-478-1162; fax: +81-53-478-1162.
E-mail address: r5245008@ipc.shizuoka.ac.jp (R. Tao).

0378-7753/$ – see front matter © 2004 Elsevier B.V. All rights reserved.
doi:10.1016/j.jpowsour.2004.04.002

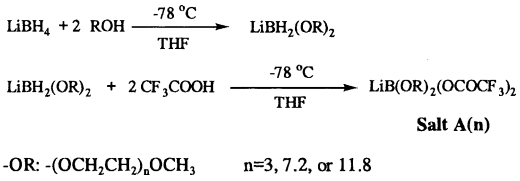

Scheme 1. Synthetic process for Salt A(*n*).

2. Experimental

2.1. Synthesis

$LiBH_4$ (2.0 M solution in tetrahydrofuran (THF), Aldrich), $LiAlH_4$ (1 M solution in THF, Adrich), trifluoroacetic acid (CF_3COOH, Kanto Chemicals), and pentafluorophenol (C_6F_5OH, Adrich) were used as supplied. Tri(ethylene glycol) monomethyl ether (TEGMME, Tokyo Kasei) was dried by distillation at reduced pressure. Poly(ethylene glycol) monomethyl ethers with molecular weights of 350 and 550 ($CH_3O(CH_2CH_2O)_{7.2}H$, PEGMME 350 and $CH_3O(CH_2CH_2O)_{11.8}H$, PEGMME 550) were dried by dry nitrogen bubbling under partial vacuum for at least 24 h and were stored over molecular sieves prior to use. THF was dried by refluxing over sodium prior to use. Unless otherwise stated, all manipulations were carried out on a dry nitrogen/vacuum line or in an argon filled glovebox for exclusion of moisture.

Lithium salts were synthesized in the process illustrated in Scheme 1. $LiBH_4$ (2 M, THF solution) 3 mL (6 mmol) dissolved in 10 mL of THF was dropped with PEGMME 350 (4.200 g, 12 mmol) diluted with 10 mL of THF at −78 °C. The mixture was allowed to recover to room temperature slowly and stirred for 4 h. The reaction mixture was then added dropwise to CF_3COOH (1.368 g, 12 mmol) solution in 10 mL of THF at −78 °C. After recovered to room temperature, the solution was stirred for another 12 h. The solvent was removed by heating at 70 °C under reduced pressure for 24 h. A clear viscous liquid, Salt A($n = 7.2$), was obtained. Complete reaction of alcohols was confirmed by the absence of –OH in IR spectra. Analytic results were as follows:

FT-IR (As_2Se_3 disc): 2876 cm^{-1} (C–H), 1714 cm^{-1} (C=O), 1468 cm^{-1} (CH_2O), 1206 cm^{-1} (C–F), 1112 cm^{-1} (C–O).

^1H NMR (300 MHz, DMSO-d_6): 3.83 ppm (t, CH_2OB), 3.51 ppm (s, CH_2CH_2O), 3.24 ppm (s, CH_3O).

In the same way, Salt A($n = 3$) and Salt A($n = 11.8$) which contain different length of oligo(ethylene oxide) chains, appeared as viscous liquids at room temperature, were obtained.

Salt B($n = 3,\ 7.2,\ 11.8$) were synthesized using the same method above described by substituting CF_3COOH with C_6F_5OH. They all appear as viscous liquids at room temperature. Analytic results of Salt B($n = 7.2$) were as follows:

FT-IR (As_2Se_3 disc): 2878 cm^{-1} (C–H), 1474 cm^{-1} (CH_2O), 1507 cm^{-1} (C_6F_5), 1109 cm^{-1} (C–O).

^1H NMR (300 MHz, DMSO-d_6): 3.85 ppm (t, CH_2OB), 3.53 ppm (s, CH_2CH_2O), 3.25 ppm (s, CH_3O).

Lithium aluminates, designated as Salt C($n = 3, 7.2, 11.8$) and Salt D($n = 3, 7.2, 11.8$) were synthesized using the

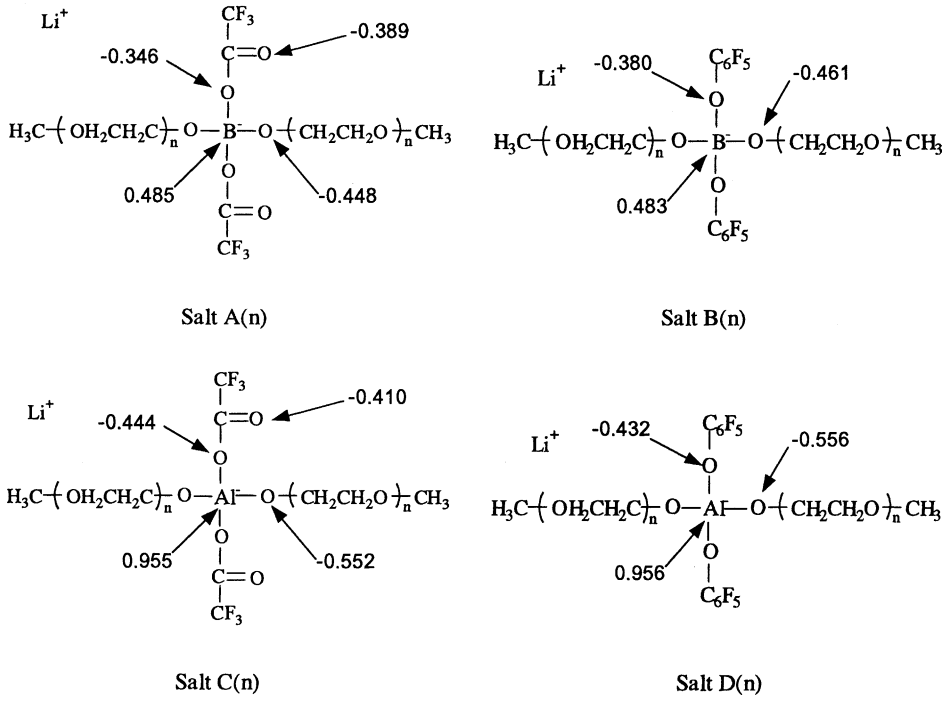

Fig. 1. Structures of synthesized lithium borates and lithium aluminates and partial charges on oxygen atoms obtained in MOPAC calculation using PM5 parameter.

same method and were reported by our laboratory before [23]. The structures of the synthesized lithium salts are presented in Fig. 1.

2.2. Characterization

IR was recorded on a Jasco FT/IR-7000 IR spectrometer. ^{1}H NMR spectra of samples in DMSO-d_6 using TMS as internal reference were obtained on a JEOL JNM-AL300 FT-NMR spectrometer. Thermal behaviors of lithium salts were determined by differential scanning calorimeter (DSC) using a Perkin-Elmer Pris 1 DSC. Heat–cool–reheat cycles were performed at a rate of 10 °C/min in a temperature range from −100 to 150 °C. All thermal events were reported for the reheating cycle. The value of glass transition temperature (T_g) was obtained from the onset of glass transition process.

Ionic conductivities of electrolytes sandwiched between stainless steel blocking electrodes were determined by ac impedance measurement in the frequency of 1 MHz to 1 Hz using a solartron 1260 frequency response analyzer and 1287 electrochemical interface. Lithium ion transference numbers (T^+) were measured for samples sandwiched between non-blocking lithium electrodes using the combined ac impedance/dc polarization method of Evans [24] modified by Abraham [25]. The electrochemical stabilities of lithium salts were determined by cyclic voltammetery using a solartron 1287 electrochemical interface at a scan rate of 10 mV/s. Stainless steel was used as working electrode, and lithium as counter and reference electrode.

Using CAChe 5.0 (Fujitsu), the structures of chemical samples were refined by performing a pre-optimization calculation in Mechanics using Augmented MM3 parameter, followed by an optimize geometry calculation in MOPAC using PM5 parameter. The partial charges were calculated for the samples in such optimized geometries.

3. Results and discussion

Salt A($n = 3, 7.2, 11.8$) and Salt B($n = 3, 7.2, 11.8$) are very viscous liquids at room temperature. Salt A($n = 11.8$) and Salt B($n = 11.8$) appear as waxy solids at low temperature (<20 °C). Thermal events of these lithium borates obtained from DSC measurement at a scan rate of 10 °C/min are summarized in Table 1.

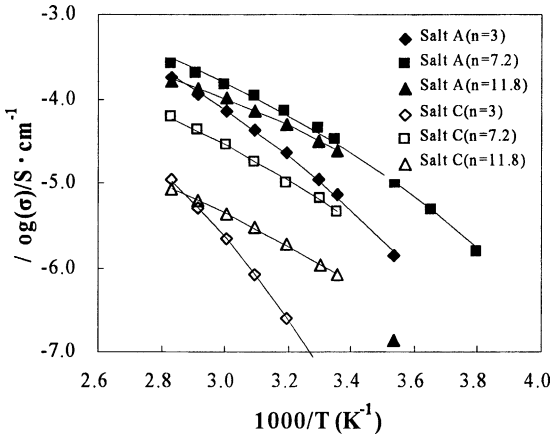

Fig. 2. Arrhenius curves for Salt A($n = 3, 7.2, 11.8$) and Salt C($n = 3, 7.2, 11.8$). The solid lines are nonlinear least-squares fits of the VTF equation to the experiment data.

Temperature dependence of ionic conductivities for Salt A and Salt B is illustrated in Figs. 2 and 3. For both Salt A and Salt B electrolyte systems, optimum ionic conductivities are observed for the borates with oligoether chains containing an average of 7.2 EO repeating units (–CH_2CH_2O–). In a typical EO chain containing lithium ion conducting electrolyte, conductivity is mainly decided by two factors: mobility of ions here dependent on the motion of EO chains, and the number of charge carriers. Salt A($n = 3$) and Salt B($n = 3$) contain high concentration of charge carriers, but large number of lithium ions which complex with oxygen atoms in EO chains during transference will remarkably stiffen ether chains reflected in higher T_g, low ionic conductivities were obtained. With the increase of the number of repeating EO units to $n = 7.2$, high mobility EO chains were obtained and enough lithium ion transference pathways were formed, which led to high ionic conductivity. Further increase of the length of ether chains leading to

Table 1
Thermal characteristics and VTF parameter data for lithium salts

Lithium salts	EO:Li$^+$	T_g(K)	T_m(K)	VTF parameters		
				$T_o = T_g - 50$ K	σ_o ($K^{-1/2}$ S/cm)	B (K)
Salt A($n = 3$)	6	222.0	–	172.0	8.44	1410
Salt A($n = 7.2$)	14.4	210.2	–	160.2	2.46	1173
Salt A($n = 11.8$)	23.6	216.6	292.3	166.6	0.42	907
Salt B($n = 3$)	6	234.7	–	184.7	10.16	1393
Salt B($n = 7.2$)	14.4	220.5	–	170.5	2.36	1163
Salt B($n = 11.8$)	23.6	227.7	291.6	177.7	0.57	922
Salt C($n = 3$)	6	257.5	–	207.5	4.36	1452
Salt C($n = 7.2$)	14.4	209.7	–	159.7	0.87	1290
Salt C($n = 11.8$)	23.6	221.2	298.5	171.2	0.04	1015

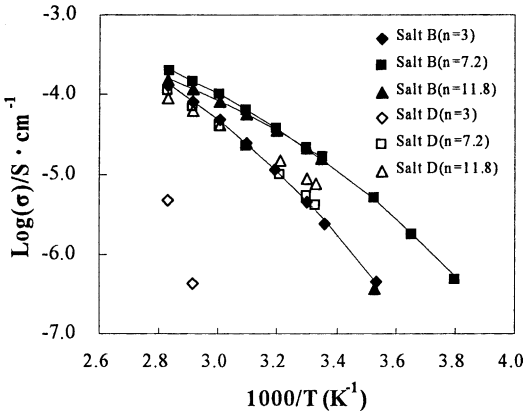

Fig. 3. Arrhenius curves for Salt B(n = 3, 7.2, 11.8) and Salt D(n = 3, 7.2, 11.8). The solid lines are nonlinear least-squares fits of the VTF equation to the experiment data.

the decrease of the number of charge carriers explained the depression of ionic conductivities for Salt A($n = 11.8$) and Salt B($n = 11.8$). Salt A($n = 7.2$) exhibited conductivity as high as 4.5×10^{-5} S/cm at room temperature (30 °C) and achieved 1.1×10^{-4} S/cm at 50 °C. At −10 °C, conductivity can also be measured as 1.5×10^{-6} S/cm.

Since Salt A(n = 7.2, 11.8) and Salt B(n = 7.2, 11.8) exhibit lower T_g than Salt A($n = 3$) and Salt B($n = 3$), respectively, better performance in conductivity at low temperature should be observed for these long ether chain containing lithium borates. Salt A($n = 7.2$) and Salt B($n = 7.2$) are more conductive at low temperature as expected. Whereas, the conductivities of Salt A($n = 11.8$) and Salt B($n = 11.8$) are still lower than those of Salt A($n = 3$) and Salt B(n = 3) at 10 °C. It can be ascribed to the crystallization of the long ether chain containing lithium borates. Endothermic peaks were observed in DSC measurement for these two salts with the corresponding T_m of 19.2 and 18.6 °C, respectively. Since lithium ion transference mainly takes place in amorous phase, a sharp drop in ionic conductivity was obtained, which can be extensively seen in typical PEO–LiX electrolyte systems.

Lithium borates exhibiting higher ionic conductivities than corresponding lithium aluminates can be obviously seen in Figs. 2 and 3. In some cases, more than one order of magnitude higher conductivities were determined for lithium borates than for lithium aluminate counterparts. It was explained by the results of geometry calculation of lithium salts in MOPAC using PM5 parameter. Ate complex center, B or Al, does not exhibit negative charge, but positive charge. The negative charge of the anion was dispersed on oxygen atoms around the ate complex center. Formation of $Li^+ \cdots O$ ion pairing structure (Fig. 4) was confirmed by MOPAC calculation. Therefore the dissociating ability of the salt is dependent on the electron donating abilities of O, i.e. partial charges on O. The calculation results are presented in Fig. 1. Oxygen atoms around the ate complex center in Salt A(n) and Salt B(n) exhibit smaller

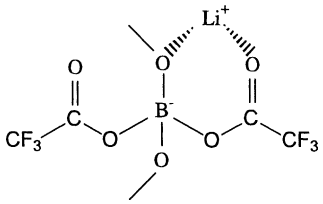

Fig. 4. Ion pairing structure formed between lithium ions and oxygen atoms in Salt A.

partial charges than counterparts in Salt C(n) and Salt D(n). Weaker ion pairing structures between Li^+ and O in lithium borates are believed, which lead to higher concentration of charge carriers and result in higher ionic conductivity. Stronger electronegativity of B than Al accounts for the smaller partial charges on O in lithium borates.

The T_g values suggest that all lithium borates are in completely amorous matrices within the temperature range studied (as to Salt A($n = 11.8$) and Salt B($n = 11.8$), $T \geqq 25$ °C). They may be described by the empirical Vogel–Tammann–Fulcher (VTF) equation [26–28].

$$\sigma T^{1/2} = \sigma_o \exp\left(\frac{-B}{T - T_o}\right)$$

where σ_o and B are constants, T_o is "equilibrium glass transition temperature", at which the free volume disappears. It is generally estimated to be about 50 °C below T_g ($T_o = T_g - 50$ K) during fitting process. The experiment data fitting well to VTF equation implies that ionic conduction in Salt A and Salt B is related to segmental motion of the oligoether chains. VTF fitting results for lithium borates and lithium aluminates are summarized in Table 1.

The VTF parameter, σ_o, relates to the number of mobile charge carriers in the electrolyte system. An increase in ion concentration should correspondingly lead to an increase in σ_o. With the decrease of the length of ether chains, σ_o does increase for both lithium borates and lithium aluminates. Parameter B is often considered as the pseudo-activation energy, representing the energy necessary for creating enough free volume for ion conduction. An increase in B by incorporation of shorter EO chains in both lithium borates and lithium aluminates is obviously seen. It can be ascribed to the increased number of pseudo-crosslinking structures formed between lithium cations and EO chains (Fig. 5) during lithium ion transference which contribute to the stiffening of segmental motion. High concentration of lithium ions

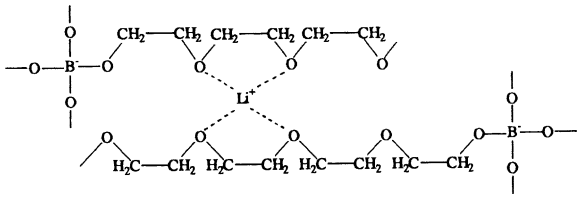

Fig. 5. Pseudo-crosslinking structures formed between lithium ions and EO chains in lithium borates.

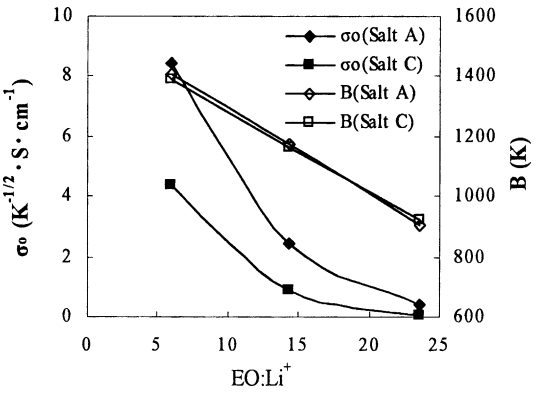

Fig. 6. The values of σ_o and B obtained from VTF fitting process for lithium salts.

will lead to low mobility of EO chains. The values of B in Table 1 are of the same magnitude as those reported for PEO systems [29]. Salt A(n) shows much larger σ_o than corresponding Salt C(n) (Fig. 6), which implies that higher concentration of charge carriers exists in lithium borates than in lithium aluminates. Since no big difference in mobility of ether chains was observed for these two systems (similar B and T_g, Fig. 6), much higher conductivities were obtained for lithium borates. Because of the close molecular weights of Salt A(n) and Salt C(n), larger number of charge carriers in Salt A(n) is believed to be the result of its higher dissociating ability, i.e. looser complex between Li^+ and O around the ate complex center existing in lithium borates. This conclusion from the VTF fitting results is in accordance with that obtained from MOPAC calculation above discussed.

In a lithium ion conducting electrolyte, both cations and anions may contribute to the total conductivity. A concentration gradient of the ions will increase in dc field which leads to the decrease of current and other safety problems [30]. Therefore, high lithium ion transference number (T^+) is greatly favored for long term lithium ion secondary batteries with good cycling performance. T^+ of synthesized lithium borates measured at 70 °C are summarized in Table 2. They are extremely higher than those normally observed in typical PEO–LiX systems (in a range of 0.2–0.4, in some cases,

Table 2
Lithium ion transference numbers of lithium borates at 70 °C

Lithium borates	Lithium ion transference numbers (T^+)
Salt A($n = 3$)	0.68
Salt A($n = 7.2$)	0.76
Salt A($n = 11.8$)	0.82
Salt B($n = 3$)	0.62
Salt B($n = 7.2$)	0.70
Salt B($n = 11.8$)	0.75

still lower than 0.1). Salt A($n = 11.8$) exhibited highest T^+ value of 0.82. T^+ of Salt A($n = 3$, 7.2) were determined to be 0.68 and 0.76, respectively. Relatively high T^+ were also observed for Salt B($n = 3$, 7.2, 11.8). It can be found that, for both Salt A and Salt B systems, T^+ was enhanced with the increase of the length of side EO chains. It was related to the decrease of the mobility of the anions. In addition, it should be realized that, although the volume of the anion of Salt A($n = 3$) is much smaller than that of Salt A($n = 11.8$), T^+ has not been greatly decreased as expected. Some other factors which contribute to the high T^+ of lithium borates are believed. As we discussed above, the movement of lithium ions in lithium borates is prompted by the motion of EO segments. Lithium ion may complex with oxygen atoms in EO chains during transference to form a psedo-crosslinking structure (Fig. 5). Although this structure is not very stable and changes with the associate-dissociate process of $Li^+ \cdots O$, it still may connect the anions into relatively large net work structures which lead to further depression of the mobility of anions.

A knowledge of electrochemical stability window is necessary for successful performance of an electrolyte in charge–discharge cycles. Fig. 7(a) and (b) show the cyclic voltammetery of Salt A($n = 7.2$) and Salt B($n = 7.2$) obtained at a sweep rate of 10 mV/s at room temperature. A cathodic peak verified between 1.0 and 2.0 V for Salt B($n = 7.2$) is probably due to the reduction of products formed in oxidation process because it is not observed in down-scans that starts at the voltage below the oxidation limit. The peaks appeared between 0.5 and −0.5 V in both

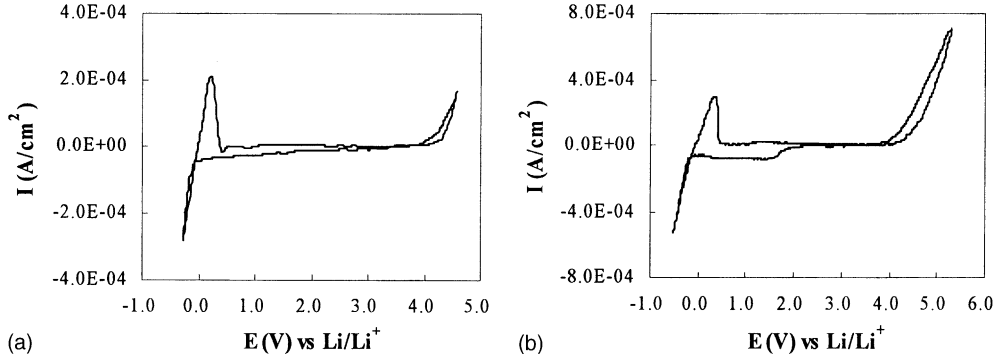

Fig. 7. Cyclic voltammetery of lithium borates at a scan rate of 10 mV/s. Working electrode: stainless steel; counter and reference electrode: Li. (a) Salt A($n = 7.2$); (b) Salt B($n = 7.2$).

voltammograms are attributed to the plating and stripping of lithium. On the anodic side, peaks corresponding to the oxidation of anions were observed. The anodic potential limits for these two lithium salts were determined to be around 4.1 V, which ensured the safe application of these borates in normal lithium ion secondary batteries.

4. Conclusion

Two types of lithium borates containing oligoether chains and electron withdrawing groups, $CF_3COO–$ or $C_6F_5O–$, were prepared. Optimum conductivities were obtained for the salts with oligoether chains in the length of 7.2 repeating EO units. High ionic conductivity, 4.5×10^{-5} S/cm at 30 °C, was determined for Salt A($n = 7.2$). Lithium borates exhibited much higher conductivities than corresponding lithium aluminates due to the weaker ion pairing structures between Li^+ and oxygen atoms in borates, which was proved by the partial charges on oxygen atoms obtained in MOPAC calculation. The transference of ions in the lithium salts was related to the segmental motion of EO chains and can be demonstrated by VTF equation. The conditions of ion motion were described by VTF parameters, σ_o and B. Larger number of charge carriers in lithium borates than in lithium aluminates was revealed by the values of σ_o. Salt A and Salt B showed much higher lithium ion transference numbers than normal PEO–LiX systems. The potential windows of the salts are also satisfactory. The battery performance of the lithium borates is under studying and will be reported separately.

References

[1] P.V. Wright, Br. Polym. J. 7 (1975) 319.
[2] D.E. Fenton, J.M. Parker, P.V. Wright, Polymer 14 (1973) 589.
[3] M.B. Armand, J.M. Chabagno, M. Duclot, in: P. Vashishta et al. (Eds.), Fast Ion Transport in Solids, Elsevier, New York, 1979, p. 131.
[4] M.B. Armand, Solid State Ion. 9–10 (1983) 745.
[5] R. Xue, C.A. Angell, Solid State Ion. 25 (1987) 223.
[6] B. Kumar, S.J. Rodrigues, S. Koka, Electrochim. Acta 47 (2002) 4125.
[7] L. Persi, F. Croce, B. Scrosati, E. Plichta, M.A. Hendrickson, J. Electrochem. Soc. 149 (2002) A212.
[8] C.J. Hawker, F. Chu, P.J. Pmery, D.J.T. Hill, Macromolecules 29 (1996) 3931.
[9] T. Itoh, M. Ikeda, N. Hirata, Y. Joriya, M. Kubo, O. Yamamoto, J. Power Sources 81–82 (1999) 824.
[10] F. Alloin, J.-Y. Sahchez, M. Armand, J. Electrochem. Soc. 141 (1994) 1915.
[11] M. Watanabe, A. Suzuki, K. Sanui, N. Ogata, J. Chem. Soc. Jpn. 14 (1986) 428.
[12] A. Bouridah, F. Dalard, D. Deroo, H. Cheradame, J.F. Le Nest, Solid State Ion. 15 (1985) 233.
[13] P.M. Blonsky, D.F. Shriver, P. Austin, H.R. Allock, J. Am. Chem. Soc. 106 (1984) 6854.
[14] D.W. Xia, D. Soltz, J. Smid, Solid State Ion. 14 (1984) 221.
[15] H.R. Allcock, S.E. Kuharcik, C.S. Reed, M.E. Napierala, Macromolecules 29 (1996) 3384.
[16] M. Leveque, J.F. Le Nest, A. Gandini, H. Cheradame, J. Power Sources 14 (1986) 23.
[17] M. Doyle, T.F. Fuller, J. Newman, J. Electrochim. Acta 39 (1994) 2073.
[18] E. Tsuchida, H. Ohno, N. Kobayashi, H. Ishizaka, Macromolecules 22 (1989) 1771.
[19] M.C. Lonergan, M.A. Ratner, D.F. Shriver, J. Am. Chem. Soc. 117 (1995) 2344.
[20] D.P. Sisca, D.F. Shriver, Chem. Mater. 13 (2001) 4698.
[21] W. Xu, M.D. Williams, A. Angel, Chem. Mater. 14 (2000) 401.
[22] T. Fujinami, A. Tokimune, M.A. Metha, D.F. Shriver, G.C. Rawshy, Chem. Mater. 9 (1997) 915.
[23] T. Fujinami, Y. Buzoujima, J. Power Sources 119 (2003) 438.
[24] J. Evans, C.A. Vincent, P.G. Bruce, Polymer 28 (1987) 2324.
[25] K.M. Abraham, Z. Jiang, B. Carroll, Chem. Mater. 9 (1997) 1978.
[26] H. Vogel, Phys. Z. 22 (1921) 645.
[27] G. Tammann, W. Hesse, Z. Anorg. Allg. Chem. 156 (1926) 245.
[28] G.S. Fulcher, J. Am. Ceram. Soc. 8 (1925) 339.
[29] S. Takeoka, H. Ohno, E. Tsuchida, Polym. Adv. Technol. 4 (1993) 53.
[30] M. Doyle, T.F. Fuller, J. Newman, Electrochim. Acta 39 (1994) 2073.